

Distributed coordination model for smart sensing applications

Luca Maggiani, Lobna Ben Khelifa, Jean-Charles Quinton, Matteo Petracca, Paolo Pagano, François Berry

▶ **To cite this version:**

Luca Maggiani, Lobna Ben Khelifa, Jean-Charles Quinton, Matteo Petracca, Paolo Pagano, et al.. Distributed coordination model for smart sensing applications. 10th International Conference on Distributed Smart Camera (ICDSC '16), Sep 2016, Paris, France. pp.110-115, 10.1145/2967413.2967438 . hal-01626468

HAL Id: hal-01626468
https://hal.science/hal-01626468

Submitted on 26 Nov 2020

HAL is a multi-disciplinary open access archive for the deposit and dissemination of scientific research documents, whether they are published or not. The documents may come from teaching and research institutions in France or abroad, or from public or private research centers.

L'archive ouverte pluridisciplinaire **HAL**, est destinée au dépôt et à la diffusion de documents scientifiques de niveau recherche, publiés ou non, émanant des établissements d'enseignement et de recherche français ou étrangers, des laboratoires publics ou privés.

Distributed coordination model for smart sensing applications

Luca Maggiani *
Scuola Superiore Sant'Anna
Pisa, Italy

Lobna Ben Khelifa
Clermont University / CNRS
Clermont-Ferrand, France

Jean-Charles Quinton
Grenoble Alpes Univ. / CNRS
Grenoble, France

Matteo Petracca
Scuola Superiore Sant'Anna
Pisa, Italy

Paolo Pagano
CNIT, National Laboratory of
Photonic Networks
Pisa, Italy

François Berry
Clermont University / CNRS
Clermont-Ferrand, France

ABSTRACT

Distributed networks of smart sensors are nowadays representing the frontier of Machine-to-Machine (M2M) interoperability. In such a scenario several challenges must be addressed in order to create effective solutions. Coordination among nodes to satisfy monitoring purposes while addressing network constraints is considered of utmost importance. In this respect, the paper proposes a novel coordination model for self-organizing smart monitoring systems. The proposed algorithm is able to autonomously retrieve event correlations from the environment in order to coordinate the nodes. By relying on temporal and spatial correlations, the proposed system can be particularly suited for Smart Camera Network (SCN) deployments where multiple cameras monitor distributed targets. Along the algorithm definition, the paper presents a performance evaluation of the proposed approach through simulations, thus evaluating the robustness of the proposed model against message losses.

1. INTRODUCTION

With nowadays improvements in information and communications technologies, more and more sensors are deployed to monitor our daily life. Traffic control sensors, access authentication systems and environmental monitoring are already widespread within our cities [1, 2]. Moreover, by overtaking the limits of a classical centralized control, sensor networks are evolving towards complete Cyber-Physical Systems (CPSs), where sensing, processing and communication policies are distributed over the network nodes. The construction, processing and transfer of semantic information can then be achieved through node-to-node communication, thus following the M2M interaction model. At a higher level, computing architectures are moving away from centralized and static deployment to autonomous entities distributed in the environment. As introduced in [3], distributed computing is challenging the computer science academia to describe and understand novel and more complex models of interactions [4]. Indeed, in designing distributed systems – and in system of systems applications as well [5] – a multi-layer formalization is needed. In this respect, we refer to the three layers shown in Fig. 1. Since in the environment a distributed sensing is performed by each sensor autonomously, a cloud of local measures – called events – is then generated. These local events are eventually analyzed and classified to recover higher level events according to a system model. The event model can be seen as a correlation map of the environment, based on the measured observations. This represents the cornerstone for higher level data aggregations and the main target of this paper. Once the model has been defined, each local event can be classified by inferring from correlations with its neighbor events, thus enabling event prediction properties.

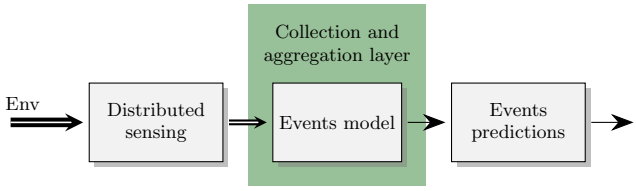


Figure 1: A distributed sensing environment formalization.

As long as the network remains relatively small, the event model can be statically defined as a function of the node calibrations. Consider a Smart City scenario where a set of Smart Cameras (SCs) trigger events in response to vehicles movements, and witness a road accident. Based on cameras placement, the event semantics can be empirically estimated due to the well-constrained scenario (e.g., vehicles directions, speed). However, along with the network growth or in case of variability (e.g., roundabout, pedestrian movements), retrieving the semantics and relationships between nodes will rapidly become more complex. Moreover, due to the often noisy input and detection glitches (false alarms),

*email: l.maggiani@sssup.it

Permission to make digital or hard copies of all or part of this work for personal or classroom use is granted without fee provided that copies are not made or distributed for profit or commercial advantage and that copies bear this notice and the full citation on the first page. Copyrights for components of this work owned by others than ACM must be honored. Abstracting with credit is permitted. To copy otherwise, or republish, to post on servers or to redistribute to lists, requires prior specific permission and/or a fee. Request permissions from permissions@acm.org.

ICDSC '16, September 12-15, 2016, Paris, France
© 2016 ACM. ISBN 978-1-4503-4786-0/16/09...$15.00
DOI: http://dx.doi.org/10.1145/2967413.2967438

a single sensor measure alone might not be reliable enough to guarantee correct higher level inferences.

Nonetheless, not all interactions are equally important: weighted connections between nodes are indeed commonplace in network based real-world problems. The concept of weighted connection topologies is a well-known method to model connection patterns for autonomous agent-based networks. In particular, in [6] the concept has been applied to characterise latent brain activities during functional Magnetic Resonance Imaging (fMRI). This led the authors to a Markov-based linear model – called Dynamic Causal Model (DCM) – to analyse and evaluate the connectivity based on observed neuronal responses. The same principle can be found in [7], where a weighted Markov chain is deployed to predict the spreading process of epidemic disease. Closer to the communication network domain, notable applications are the *Page Rank* algorithm by Google [8] and the consensus and averaging algorithms as in [9]. The former evaluates the web page importance as the capability to connect other high quality nodes in its surrounding. The latter represents instead a state-of-the-art proposal for SCNs, where a combination of measures and distributed agreement algorithms are deployed to enforce the consensus formation [10–14].

Our proposed distributed coordination model addresses the aforementioned issues by leveraging self-organizing node interactions. These interactions are used to: (i) make the system adapt to changing environment conditions and to unpredicted events, (ii) improve the detection reliability by aggregating conform events, (iii) improve the system robustness against node malfunction [9] and detection glitches. The proposed distributed coordination model is inserted into the collection and aggregation layer, as in the middle step in Fig. 1. In other words, we made the assumption that the distributed system – e.g., a SCN – is able to generate higher level events from collected local measures. These measures are then collected and semantically aggregated by the *Event model* which formally defines the interaction patterns. The model produces the most-probable node interactions, according to spatial and temporal correlations mesured between nodes.

The remainder of the paper is organized as follows. The mathematical notations and the system description are presented in the next section. In Section 3 the proposed model is presented. Section 4 shows the evaluation results. Finally, the conclusion is drawn and future directions are described in Section 5.

2. SYSTEM DESCRIPTION

In the considered scenario measures are autonomously performed by each node over its well-behaved local surroundings. The system environment results then in a manifold space composed by aggregating overlapped local measurement spaces. Each node is defined with the identifier C_n and its relative state s_n. The state s_n represents the node rank within the network and its contribution to the distributed coordination. The node state vector at time k is defined as:

$$\underline{s}^k = \{s_1, \dots, s_N\}^k \tag{1}$$

where N is the number of nodes at time k. Moreover, each node describes its surroundings by defining a *visibility* range, namely the maximum distance within the target is detected by the node itself. On first approximation omnidirectional visibility spaces and uniform detection ranges are considered. This limit is initially introduced to simplify the mathematical formalism where further investigations are considered as future perspectives. The targets are moving entities

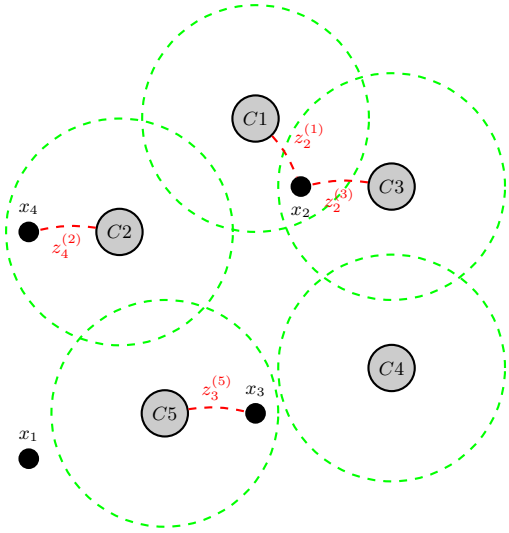


Figure 2: An instance of the system environment space, with visibility ranges as dashed circles.

which are defined by their signatures, e.g., visual features, positions, speeds, trajectories. The target vector is defined as:

$$\underline{x}^k = \{x_1, \dots, x_M\}^k \tag{2}$$

where each component represents a target signature and M the number of targets that appear at time k. The causal evolution of $\underline{x}^k$ is described as:

$$\underline{x}' = G^k(\underline{x}^k) \tag{3}$$

where $G^k(\cdot)$ is a Markov chain process of the vector $\underline{x}^k$ and x' represents the target at interval $k+1$. In particular, G^k is a memory-less stochastic process with unobservable states (as known as Markov assumption). As a consequence, the behaviour of the x_m with $m \in M$ target at time k can be evaluated as the probability distribution of the previous $k-1$ sample rather than the complete set of the target samples $\underline{x} = \{x^{k-1}, x^{k-2}, \dots\}$.

The targets are observed by the nodes through measures (if targets reside in the visibility range). Each measure is an approximation of the target features with respect to a specific node at one specific time interval. The observation vector is therefore defined as follows:

$$\underline{z}^k = \{z_1, \dots, z_M\}^k \tag{4}$$

where M still considers the available targets at time k. Since each node performs its own measures, multiple appearances of $\underline{x}^k$ could exist. In particular, from the node $C1$ the observation vector is defined as:

$$\underline{z}^{(1,k)} = \{z_1^1, \dots, z_M^1\}^k \text{ as seen from C1} \tag{5}$$

For instance, in Fig. 2 a system environment space is depicted. Here five nodes are instantiated $C1, \cdots, C5$ with

their states $s_1, \cdots, s_5$ respectively. With this respect, targets $x_1, \cdots, x_4$ are arbitrarily placed and are moving following a deterministic trajectory. The $z_4^{(2)}$ measure refers to the x_4 target being detected inside the visibility area of $C2$. Since x_2 belongs to the $C3$ and $C1$ visibility areas, double target measures are then retrieved. Due to the noisy environment and to the different spatial conditions, these measures are only ideally equivalents while they present some degrees of correlation. The distributed coordination model, which is the main contribution of this paper, is then defined as:

$$\underline{s}' = F^k(\underline{s}^k, \underline{z}^k) \tag{6}$$

where $F^k(\cdot)$ represents the state transition function. The state vector $\underline{s}'$ at time sample $k+1$ becomes then a function of the previous state vector $\underline{s}^k$ and of the performed measures $\underline{z}^k$. Through local observations, the aim of the coordination is to reinforce the nodes interactions by approximating the G^k function with the a-posteriori evaluation F^k. In the next section, the structure of F^k is analysed by proposing a novel methodology.

3. DISTRIBUTED NETWORK MODEL

According to the Eq. 6, our discrete time model is formalized as a function of it previous state $\underline{s}^k$ and the input stimuli vector applied to the system $\underline{z}^k$. Assuming a bi-linear Taylor transformation of F, in Eq. 7 the dependencies in s and z are expressed.

$$\frac{ds}{dt} = \frac{\partial F}{\partial s}|_z ds + \frac{\partial F}{\partial z}|_s dz + \frac{\partial^2 F}{\partial s \partial z} ds dz \tag{7}$$

where

$$A = \frac{\partial f}{\partial s}|_z \quad \text{and} \quad B = \frac{\partial f}{\partial z}|_s \quad \text{and} \quad C = \frac{\partial A}{\partial z} dz \tag{8}$$

Finally, in Eq. 9 the system model equations are expressed. The vector notation is derived from the Eq. 6 and makes it suitable to multiple node instances. The scalar values A, B, C as in Eq. 7 become square matrices $\mathbf{A}, \mathbf{B}, \mathbf{C}$ and s' the state vector $\underline{s}'$. The Eq. 9 also expresses the temporal dependence of the $\mathbf{A}'$ term as the combination of the $\mathbf{A}$ and $\mathbf{C}$ of the previous iteration.

$$\begin{aligned} \underline{s}' &= \mathbf{A}\underline{s} + \mathbf{B}\underline{z} \\ \mathbf{A}' &= \mathbf{A} + \mathbf{C} \end{aligned} \tag{9}$$

The system dynamic $\underline{s}'$ is driven by the input measures $\underline{z}$ in two separate contributions: (i) the response to direct stimuli through $\mathbf{B}$ matrix or (ii) the induced interactions according to the $\mathbf{C}$ matrix (as Eq. 8). The $\mathbf{A}$ matrix results from the Bayes assumption, where the next state depends on the a-posteriori probability of interaction. The matrix $\mathbf{B}$ instead represents observation space and the source term in the system. Finally, the dynamic and time-changing term $\mathbf{C}$ adds to the state matrix the induced connectivity as results of interaction pattern in the environment (it creates/removes connections coupling). In the following, the $\mathbf{A}, \mathbf{B}, \mathbf{C}$ contributions are considered to evaluate their effect on the state transition function F^k.

3.1 Stochastic connectivity

According to Eq. 9, the $\mathbf{A}$ matrix represents the next-state transition probability from the vector state $\underline{s}$. This is modeled as a stochastic adjacency matrix and contains $N \times N$ non-negative entries for every possible state transition. For a given state s_n related to the $n-th$ node, the interactions with the others can be expressed as a linear combination of the row elements of $\mathbf{A}$. These interactions are described as unidirected graphs, where connections are expressed as edges and nodes as vertex. The existence of interaction is revealed by a non-zero probability p_{ij} between the source node i and the target node j.

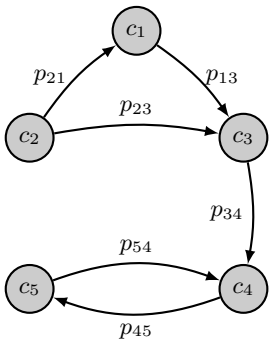


Figure 3: A connectivity graph example based on Fig. 2.

For instance, assume that Fig. 3 represents the connectivity graph of the system in Fig. 2. A connection exists from $C3$ towards $C4$ but no interaction is defined between $C2$ and $C5$ though. The existence of an interaction is due to the previous measured activities (e.g., events correlation) between nodes. This concept, borrowed from the biology [15] and social network [16] studies, allows to represent distributed networks as functional connectivity between entities. An active communication is therefore defined by A as a probability distribution and it is not related to the physical network topology – e.g., Received Signal Strength Indicator (RSSI). For instance, far apart nodes with low RSSI unlikely measures correlated events unless considering complex environment configuration. On the other side, nodes with high signal strengths might not automatically showing correlation between their measures. Thus, signal structure features can not be used to assess event correlations but they might rather considered as a complementary information to the model.

According to Eq. 9, A is a right stochastic matrix, with each row summing to 1. This property induces that the state transitions are balanced between the outgoing transitions (p_{ij} with $i \neq j$) and the steady state p_{ii} one. The lower p_{ii}, the higher is the importance of interactions. This results in a trade-off between steady state and transitions which depends on the importance given to communications rather than on the measures available in the node itself. In Eq. 10 the network connections shown in Fig. 3 are described.

$$A = \begin{pmatrix} p_{11} & 0 & p_{13} & 0 & 0 \\ p_{21} & p_{22} & p_{23} & 0 & 0 \\ 0 & 0 & p_{33} & p_{34} & 0 \\ 0 & 0 & 0 & p_{44} & p_{45} \\ 0 & 0 & 0 & p_{54} & p_{55} \end{pmatrix} \tag{10}$$

At system initialization, the relevant communication patterns between nodes is not usually known. The stochastic matrix A is therefore initialized to uniformly distributed probabilities. This means that each interaction is equally important and any distinction between them is to be later

inferred. Thus, according to the Eq. 9 and in absence of the source term, the system is in a steady state (the state vector $\underline{s}$ is null). Through observations relevant correlations are collected and used to update the stochastic model of A. This event gathering phase (as in Fig. 1) is an on-line process that continuously measures and adapts the system response towards the likelihood expectation.

3.2 Observation matrix

While temporal event correlation drives the stochastic and the induced connectivity matrices, the spatial correlations are considered for measures. According to Eq. 11, the observation matrix B represents the observation space, as composed by the multiple measures of the target vector $\underline{z}$ performed by the N nodes.

$$\mathbf{B} = \{z_m^n\}^k \quad n \in \{1, N\}, \quad m \in \{1, M\} \tag{11}$$

In Fig. 4 the relationship between the observation matrix and the target vectors is shown. Since physical systems are unlikely fully observable, the B is considered as a sparse matrix. A zeroed column i means that the target x_i is not visible from the system therefore the relative measures are not considered. Each element of B represents how much two

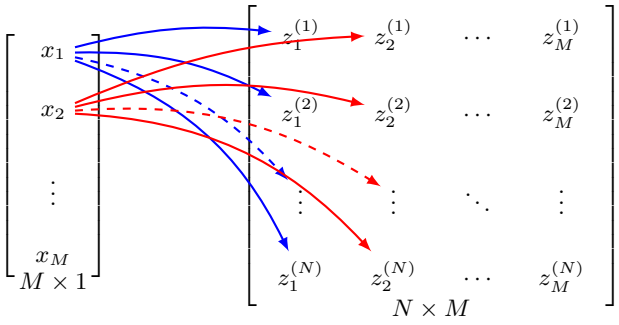


Figure 4: The relationship between the target vector $\underline{x}$ and the observation matrix B.

measures are correlated within the same temporal interval k. This usually results in a geometrical evaluation between visibility ranges. The way of deriving it actually depends on the physical phenomenon under measure. For instance, in SCNs the spatial correlations are related the cameras' field of views intersections and can be evaluated using affine region detectors [17] or the Simultaneous Localization And Mapping (SLAM) technique [18]. For proprioceptive sensors, e.g. vibration, temperature, spatial correlation is rather evaluated with correlation indexes, such as Moran's I [19].

3.3 Induced connectivity

Given a set of events occurred within the network, nodes that are showing relevant event correlations are establishing active communications among them. Each node is modeled as an autonomous agent which tries to learn the optimal neighbor selection policy from its history of interaction. Since the environment has been defined as a Markov process (according to G^k), events correlations are meaningful information to reveal repetitive patterns of behaviour. In Eq. 12, a simplified version of the Q-Learning algorithm [20] has been used to evaluate the induced connectivity as the $\mathbf{C}$ term.

$$\mathbf{C} = \alpha(\mathbf{R} - \mathbf{A}) \tag{12}$$

where $\alpha \in \mathbb{R}[0, 1)$ is the learning rate, R is the reward observed after validating the prediction. The elements of $\mathbf{C}$ can be computed as follows:

$$c_{ij} = \alpha(r_{ij} - p_{ij}) \tag{13}$$

where p_{ij} is the likelihood that the event (measure of a target) evolves from the camera i to the camera j (see Eq. 10). The reward term r_{ij} is related to the temporal correlation analysis between available measures from camera i to j. This factor is evaluated using a Gaussian probability distribution $\mathcal{N}_{ij}(\tau_{m,ij}, \sigma_{ij}^2)$ centred at the delay time expectation $\tau_{m,ij}$ between nodes. For instance, if a target x_1 is detected from the node $C1$ and then from the node $C2$, the delay time as τ_{12} can be measured. If this target is periodically detected between the nodes, an expected delay time $\tau_{m,12}$ can be also estimated. Since then, in order to evaluate whether nodes are temporally correlated or not, the measured τ_{12} is compared to the $\tau_{m,12}$ through the time delay distribution. The closer is τ_{12} to the model average, the higher correlation probability results. Then higher correlation turns to higher r_{12} reward. By iteratively updating the τ_m averages and giving the likelihood probability of correlation, the nodes strengthen their coordination in case of correlated event and vice versa. In Eq. 14 the reward r_{ij} computation is expressed as function of the standard deviation σ_{ij}.

$$r_{ij} = \begin{cases} +1 & \text{if } \tau_{ij} - \tau_{m,ij} \leq \sigma_{ij} \\ -1 & \text{if } \tau_{ij} - \tau_{m,ij} \geq 2\sigma_{ij} \\ 0 & \text{else} \end{cases} \tag{14}$$

Since the probability distributions $\mathcal{N}_{ij}$ are on-line computed, the reward evaluations are continuously updated to meet environmental variations and to detect abnormal events that might occur. The third case in Eq. 14, which brings a neutral reward, has been introduced as an hysteresis guard that prevents reward oscillations.

4. EVALUATION

In this section, a simple smart sensing application is considered to evaluate the methodology presented in Section 3. In the proposed evaluations, we show how the system is autonomously coordinating the nodes interactions as results of specific event patterns. The system is composed of a set of nodes which are able to perform measurements whitin their own visibility range and to communicate with others. For instance, this would be the case of a distributed video-surveillance deployment, where each node is a SC able to detect visual targets. No knowledge about node positions, visibility ranges and neighborhoods are needed during system setup.

The simulations are performed using the discrete event simulator OMNeT++ [21], installed in a PC workstation. The main goal of these preliminary evaluations is to show the effect of nodes coordination to reach a stable state without assumptions on the setup environment. Moreover, the system is also evaluated in term of robustness with respect to message losses (as an uniform density of probability of losing messages) and to glitches detection (which causes false alarms).

The state transition probabilities p_{ij} are initially setup to $1/N$ (where N is the number of the available nodes, as in Eq. 1). Assuming this uniform probability results in an initially unbiased state transition policy. Moreover, the target

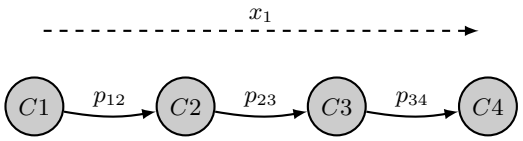


Figure 5: Aligned nodes configuration.

trajectories are deterministic with constant motion speeds and the observation matrix $\mathbf{B}$ is considered equivalent to an identity matrix. In the followings, the state transition probability is then computed according to Eq. 13 as:

$$p'_{ij} = p_{ij} + \alpha(r_{ij} - p_{ij}) \tag{15}$$

where α is fixed to 0.2 and the reward is computed as in Eq. 14. The expected delays time $\tau_{m,ij}$ are evaluated as a weighted moving average over the last measures by each node in order to reduce the effect of outliers.

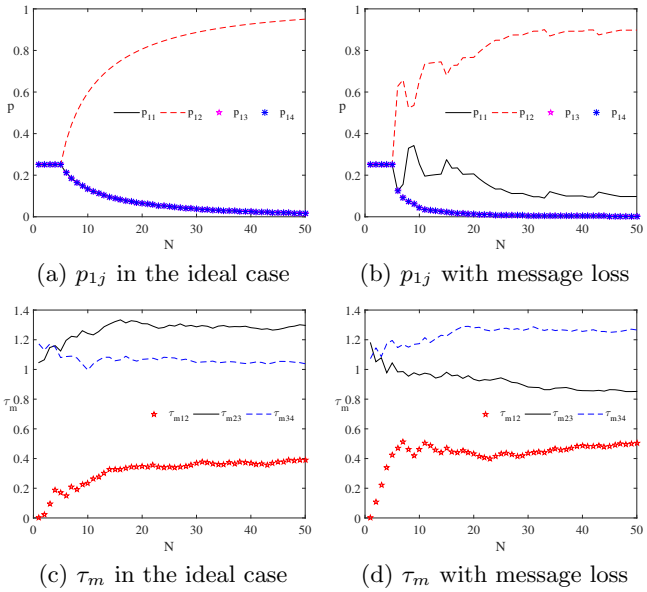
4.1 Aligned nodes

In Fig. 5 the first setup configuration is shown. In particular, the nodes $C1, \cdots, C4$ are aligned to the target x_1 trajectory. The target is repeatedly following the same path, from the left to the right side (the dashed line in Fig. 5).

In Fig. 6 the simulation results are shown for 50 time samples. In particular, in Fig. (a) the state transition probabilities p_{1j} from node $C1$ are computed. The p_{1j} are computed according to Eq. 9 and initially setup to 1/4. After the start-up phase, the p_{12} probability increases while p_{13}, p_{14} decrease. Also p_{11} decreases as well as p_{12} converges towards 1. In Fig. (b), the expected time $\tau_{m_{ij}}$ are shown. These time references are continuously updated with new measures. As expected, as long as the system converges towards stable transition probabilities, the τ_m indexes are stable as well. In Fig. 6c and 6d the same system configuration is evaluated in case of random communication failures. Although the target is still following the same trajectory, the system response is slower than in the ideal case but yet reaches a stable state. It worth noting that the fluctuation of p_{12} due to the communication noise are absorbed by the steady state s_{11} through p_{11}. This means that if the node experiences message losses, its state transition probability decreases in favor of the steady state probability.

4.2 Non-aligned nodes

The second configuration introduces nodes $C1, \cdots, C4$ with a non aligned configuration. In this case, also the target x_1 trajectory might change between the two dashed lines in Fig. 7. Once again, the evaluation is presented in the Fig. 8 as function of the stochastic connectivity and the expected delay time τ_m seen from the node $C2$. With respect to the other case, the environment presents more variability thus resulting in more unstable behaviour. Therefore the simulation in the ideal case and in case of message loss are extended to 100 and 1000 time samples respectively. Since the trajectory path is randomly chosen between the two available, in Fig. 8a both p_{23} and p_{24} are varying accordingly with the current path. These transition probabilities asymptotically converges to the decision rate between trajectories. For these simulations a uniform probability rate has been used, thus both p_{23} and p_{24} asymptotically reaches 0.5. Although the trajectories are randomly chosen, the target movements are still deterministic. This explains the relative stability



(a) p_{1j} in the ideal case (b) p_{1j} with message loss

(c) τ_m in the ideal case (d) τ_m with message loss

Figure 6: The system dynamic seen from node $C1$ in the aligned nodes setup.

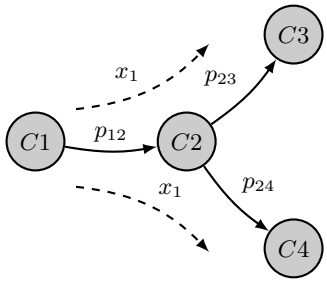


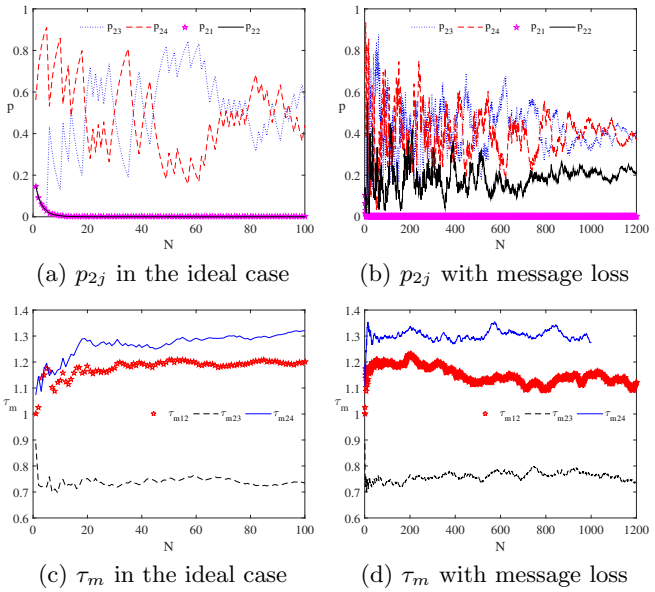
Figure 7: Non-aligned nodes configuration.

of the time delay expectations τ_m in Fig. 8b with respect to the state transition rates. As long as the environment presents event correlation patterns, the system is able to extract stable time delay expectations. In Fig. 8c the message loss impact are shown for the non aligned configuration. As expected, the steady state probability p_{22} is absorbing the system fluctuation by reducing the state transition rate. As a result, the system takes more time to converge (the time scale has been extended to 1000 samples) as previously seen in Fig. 6c. No qualitative variations are instead evaluated in Fig. 8d with respect to the ideal case in Fig. 8b.

5. CONCLUSIONS

In the paper a novel distributed coordination model for smart sensing application has been proposed. The presented methodology is suitable for autonomous smart sensing application, where the nodes are arbitrarily placed in the environment. With respect to standard sensor deployments, a coordination algorithm simplify the system installation and reduces the maintenance. The preliminary evaluations proposed in this paper shows robustness with respect to message losses or detection glitches.

Many are the future perspectives. First of all, we will further simulate the model with more complex networks with different experimental conditions. Then the algorithm will



(a) p_{2j} in the ideal case (b) p_{2j} with message loss

(c) τ_m in the ideal case (d) τ_m with message loss

Figure 8: The system dynamic seen from node $C2$ in the non-aligned nodes setup.

be evaluated in a physical SCN scenario, where node coordination can be used as a distributed target tracking application.

Acknowledgment

This work has been partially sponsored by the French government research program "Investissements d'avenir" through the IMobS3 Laboratory of Excellence and by the the European Union under the European Regional Development Fund (ERDF).

6. REFERENCES

[1] Daniele Miorandi, Sabrina Sicari, Francesco De Pellegrini, and Imrich Chlamtac, "Internet of things: Vision, applications and research challenges," *Ad Hoc Networks*, vol. 10, no. 7, pp. 1497 – 1516, 2012.

[2] Charith Perera, Chi Harold Liu, Srimal Jayawardena, and Min Chen, "A survey on internet of things from industrial market perspective," *IEEE Access*, vol. 2, pp. 1660–1679, 2014.

[3] Dan Chalmers, Matthew Chalmers, Jon Crowcroft, Marta Kwiatkowska, Robin Milner, Eamonn O'Neill, Tom Rodden, Vladimiro Sassone, and Morris Sloman, "Ubiquitous computing: experience, design and science," in *Ubiquitous Computing: 8th International Conference*, 2006.

[4] Morris Sloman, Martyn Thomas, Karen Sparck-Jones, Jon Crowcroft, Marta Kwiatkowska, Paul Garner, Nicholas R Jennings, Vladimiro Sassone, Eamonn O'Neill, Michael Wooldridge, et al., "Discussion on robin milner's first computer journal lecture: ubiquitous computing: shall we understand it?," *The Computer Journal*, 2006.

[5] Dominik Wachholder and Chris Stary, "Enabling emergent behavior in systems-of-systems through bigraph-based modeling," in *System of Systems Engineering Conference (SoSE), 2015 10th.* IEEE, 2015, pp. 334–339.

[6] Karl J Friston, Joshua Kahan, Bharat Biswal, and Adeel Razi, "A dcm for resting state fmri," *Neuroimage*, vol. 94, pp. 396–407, 2014.

[7] Eugenio Valdano, Luca Ferreri, Chiara Poletto, and Vittoria Colizza, "Analytical computation of the epidemic threshold on temporal networks," *Physical Review X*, vol. 5, no. 2, pp. 021005, 2015.

[8] Lawrence Page, Sergey Brin, Rajeev Motwani, and Terry Winograd, "The pagerank citation ranking: bringing order to the web.," 1999.

[9] Reza Olfati-Saber, J Alex Fax, and Richard M Murray, "Consensus and cooperation in networked multi-agent systems," *Proceedings of the IEEE*, vol. 95, no. 1, pp. 215–233, 2007.

[10] Uğur Murat Erdem and Stan Sclaroff, "Event prediction in a hybrid camera network," *ACM Trans. Sen. Netw.*, vol. 8, no. 2, pp. 16:1–16:27, Mar. 2012.

[11] Dragana Bajovic, Joao Xavier, José MF Moura, and Bruno Sinopoli, "Consensus and products of random stochastic matrices: Exact rate for convergence in probability," *Signal Processing, IEEE Transactions on*, vol. 61, no. 10, pp. 2557–2571, 2013.

[12] Prabhu Natarajan, Pradeep K Atrey, and Mohan Kankanhalli, "Multi-camera coordination and control in surveillance systems: a survey," *ACM Transactions on Multimedia Computing, Communications, and Applications (TOMM)*, vol. 11, no. 4, pp. 57, 2015.

[13] Aiping Wang, "Event-based consensus control for single-integrator networks with communication time delays," *Neurocomputing*, 2016.

[14] Guillem Martínez-Cánovas, Elena Del Val, Vicente Botti, Penélope Hernández, and Miguel Rebollo, "A formal model based on game theory for the analysis of cooperation in distributed service discovery," *Information Sciences*, vol. 326, pp. 59–70, 2016.

[15] Klaas Enno Stephan and Karl J Friston, "Models of effective connectivity in neural systems," in *Handbook of Brain Connectivity*, pp. 303–327. Springer, 2007.

[16] Mehmet C Vuran, Özgür B Akan, and Ian F Akyildiz, "Spatio-temporal correlation: theory and applications for wireless sensor networks," *Computer Networks*, vol. 45, no. 3, pp. 245–259, 2004.

[17] Krystian Mikolajczyk, Tinne Tuytelaars, Cordelia Schmid, Andrew Zisserman, Jiri Matas, Frederik Schaffalitzky, Timor Kadir, and Luc Van Gool, "A comparison of affine region detectors," *International journal of computer vision*, vol. 65, pp. 43–72, 2005.

[18] Randall Smith, Matthew Self, and Peter Cheeseman, "Estimating uncertain spatial relationships in robotics," in *Autonomous robot vehicles*, pp. 167–193. Springer, 1990.

[19] Patrick AP Moran, "Notes on continuous stochastic phenomena," *Biometrika*, vol. 37, no. 1, pp. 17–23, 1950.

[20] Christopher John Cornish Hellaby Watkins, *Learning from delayed rewards*, Ph.D. thesis, University of Cambridge England, 1989.

[21] András Varga, "Omnet++ discrete event simulation system," 2008.